



ELSEVIER

Available online at www.sciencedirect.com



Nuclear Physics B Proceedings Supplement 00 (2021) 1–7

---



---

**Nuclear Physics B  
Proceedings  
Supplement**


---



---

## CP-violating Higgs boson production in association with three jets via gluon fusion

Francisco Campanario<sup>a,b,1</sup>, Michael Kubocz<sup>b,c</sup><sup>a</sup>Theory Division, IFIC, University of Valencia-CSIC, E-46980 Paterna, Valencia, Spain<sup>b</sup>Institute for Theoretical Physics, KIT, 76128 Karlsruhe, Germany.<sup>c</sup>Institut für Theoretische Teilchenphysik und Kosmologie, RWTH Aachen University, D52056 Aachen, Germany

---

### Abstract

In these proceedings, we present results for Higgs production at the LHC via gluon fusion with triple real emission corrections and the validity range of the heavy-top effective theory approximation for this process. For a general  $CP$ -violating Higgs boson, we show that bottom-quark loop corrections in combination with large values of  $\tan\beta$  significantly distort differential distributions.

**Keywords:** Collider Physics, Higgs plus jets

---

### 1. Introduction

Higgs production in association with two jets via gluon fusion (GF) is a promising channel to measure the  $CP$ -properties of the recently found new scalar boson [1, 2] with mass of 126 GeV. The azimuthal angle correlations lead to a distinguishable spectrum [3, 4] sensitive to (1) the  $CP$ -nature of the Higgs particle, shifting the positions of the minima/maxima, (2) the Yukawa couplings, which change the normalization of the cross sections, (3) parameters in theories beyond the Standard Model (BSM), like  $\tan\beta$ , which can significantly distort phenomenologically important differential distributions. Higgs production in association with two jets via GF at leading order (LO) is a loop induced process of order  $\alpha_s^4$ . The LO corrections for a scalar Higgs particle were computed in Ref. [3] and for a general  $CP$ -violating Higgs in Ref. [5]. Predictions within an effective theory approximation are known at NLO accuracy [6, 7]. They reduce the scale uncertainties considerably. However, the validity of these predictions are restricted to Higgs/jet transverse momentum and/or for

Higgs masses lower than the top-quark mass. Furthermore, this approximation provides no predictions for bottom-quark induced loop contributions which can be relevant in BSM scenarios, e.g. due to a strong enhancement via  $\tan\beta = v_u/v_d$ , the ratio of two vacuum expectation values, appearing in two Higgs doublet models (2HDM), like the Minimal Supersymmetric Standard Model.

In these proceedings, we show results for the production of a general  $CP$ -violating Higgs boson in association with three jets via GF at LO beyond the heavy top-quark limit approximation, presented in Ref. [8]. Results, for the  $CP$ -even scalar case were given in Ref. [9]<sup>2</sup>. This process is an essential piece to compute the full NLO corrections of Higgs plus two jet production process via GF. Focusing particularly on the  $gg \rightarrow ggg\Phi$  sub-process, being enhanced by large gluonic PDFs at the LHC, we study the validity of the effective theory approximation and the possible modifications of the azimuthal angle correlations due to the presence of additional radiation. Additionally we inves-

---

<sup>1</sup>Speaker. Prepared for the 37th International Conference on High Energy Physics (ICHEP 2014), 2-9 Jul 2014, Valencia, Spain.

---

<sup>2</sup>Recent results within the effective theory approach are also available at NLO in Ref. [10] for a  $CP$ -even scalar Higgs boson and for the electroweak induced process in Ref. [11]

tigate bottom-quark loop contributions in combination with large values  $\tan\beta$ .

Sections 2 and 3 describe briefly the theoretical background and details of the calculational set up. Numerical results are presented in Sect. 4 and conclusions in Sect. 5.

## 2. Theoretical Framework

A general  $CP$ -violating Higgs boson,  $\Phi$ , formed by a mixing of a  $CP$ -odd,  $A$ , and a  $CP$ -even Higgs,  $H$ , state,

$$\Phi = H \cos \alpha + A \sin \alpha, \quad (1)$$

can be described via the Lagrangian

$$\mathcal{L}_{\text{Yukawa}} = \bar{q}(y_q \cos \alpha + i\gamma_5 \tilde{y}_q \sin \alpha) q \Phi, \quad (2)$$

where  $y_q$  and  $\tilde{y}_q$  denote the Yukawa couplings of the  $CP$ -even and  $CP$ -odd components to fermions  $q$ . In the SM, the smallness of the bottom-quark mass,  $m_b$ , leads to a suppression of the corresponding Yukawa coupling,  $y_b^{\text{SM}} = m_b/v$ , with  $v = 246$  GeV, the SM vacuum expectation value. Thus, corrections with bottom-quarks provide negligible contributions in gluon fusion production modes. The remaining top-quark loop effects can be therefore described within certain limits in a simplified form by the heavy top-quark mass limit approach. In this limit, top-quark loops are replaced by effective Higgs – gluons vertices, reducing the complexity of the calculations considerably. The corresponding Lagrangian for a general  $CP$ -violating Higgs is given by

$$\mathcal{L}_{\text{eff}} = \frac{\alpha_s}{12\pi m_t} \left( Y_t G_{\mu\nu}^a G^{a\mu\nu} + \tilde{Y}_t \frac{3}{2} G_{\mu\nu}^a \tilde{G}^{a\mu\nu} \right) \Phi, \quad (3)$$

where  $G_{\mu\nu}^a$  represents the gluon field strength and  $\tilde{G}^{a\mu\nu} = 1/2 G_{\rho\sigma}^a \epsilon^{\mu\nu\rho\sigma}$  its dual. The generalized Yukawa couplings  $Y_t = \text{FF}_H y_t \cos \alpha$  and  $\tilde{Y}_t = \text{FF}_A \tilde{y}_t \cos \alpha$  include also form factors ( $\text{FF}_{H,A}$ ). They are derived from the partial decay width of the Higgs boson to two gluons and are therefore proportional to triangle fermion-loops, re-introducing back missing quark dependencies [12, 13]. Their explicit form can be found in Ref. [8]. As mentioned before, the validity of the heavy top-quark limit is restricted to Higgs masses and values of the transverse momentum lower than the top-quark mass. Additionally, in a 2HDM of type II, for large values of  $\tan\beta$ , the Yukawa couplings with bottom-quarks receive strong enhancement and therefore should be taken into account. In the effective theory approach, these contribution are, of course, absent. The up- and

down-type Yukawa couplings for the  $CP$ -odd components are given by,

$$\tilde{y}_u^{\text{II}} = -\frac{\cot\beta}{v} m_u \quad \text{and} \quad \tilde{y}_d^{\text{II}} = -\frac{\tan\beta}{v} m_d, \quad (4)$$

where the SM-like vacuum expectation value  $v = \sqrt{v_d^2 + v_u^2} = 246$  GeV and  $\tan\beta = v_u/v_d$  are functions of the two vacuum expectation values. Henceforth, in our study of  $\Phi jjj$  production, we will include bottom-quark loop corrections to investigate their phenomenological effects and test the validity bounds of the effective theory approximation.

## 3. Calculational set up

In  $\Phi jjj$  production, there are four contributing subprocesses,

$$\begin{aligned} qq &\rightarrow qqg\Phi, & qQ &\rightarrow qQg\Phi, \\ qg &\rightarrow qgg\Phi, & gg &\rightarrow ggg\Phi, \end{aligned} \quad (5)$$

together with the corresponding cross-related processes, which are not written here explicitly. We show results for the purely gluonic channel, which is enhanced by the large gluon flux at the LHC. This sub-process is also the most complicated one, because it contains massive hexagon one-loop diagrams, allowing us to test the numerical stability of our program. Note that the LO contribution involves a  $2 \rightarrow 4$  one-loop  $\times$  one-loop calculation, thus, being subjected to numerical instabilities of different kinds [14]. The details of our calculation and the performed checks can be found in Refs. [8, 9]. Here, we provide a summary with the main features.

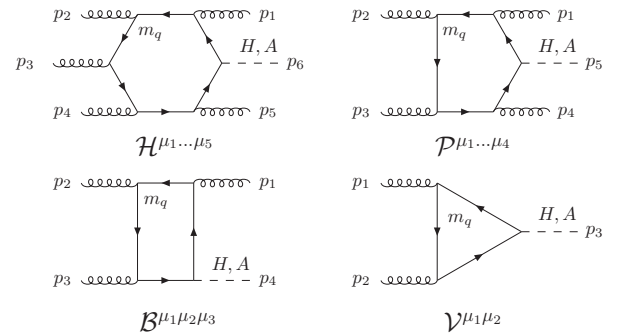


Figure 1: Master Feynman diagrams

Eight master Feynman diagrams (Fig. 1) involving four  $CP$ -even and four  $CP$ -odd Higgs couplings to fermions were computed with the in-house framework described in Ref. [15] – the attached gluons are considered to be off-shell vector currents, which allow the addition of

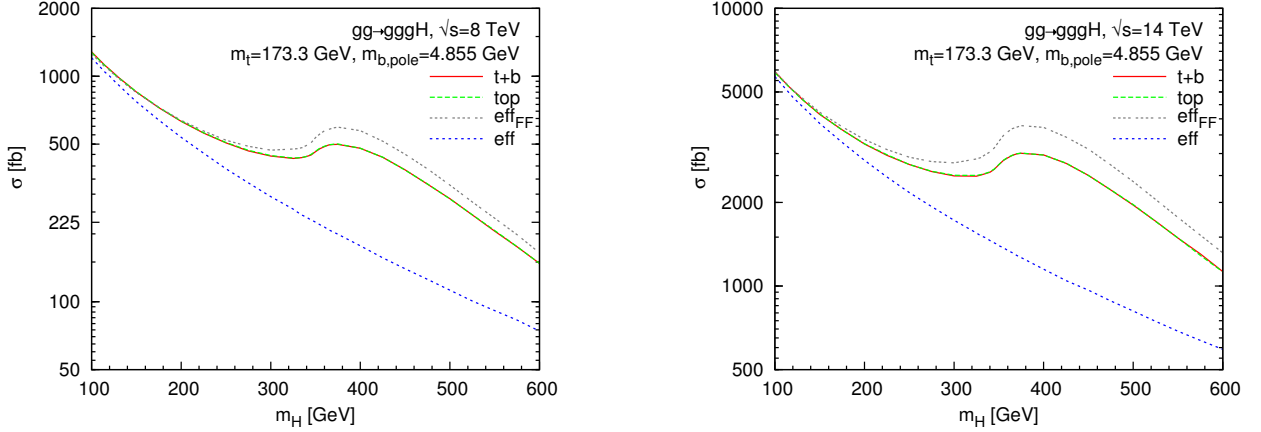


Figure 2: Cross section of the  $gg \rightarrow gggH$  scattering sub-process as a function of Higgs boson mass for c.m. energies of 8 TeV and 14 TeV. Both panels show the effective (with and without FF) and the full theory contributions. The applied cuts are discussed in the text in more detail.

further participating gluons. For this, we exploit the effective current approach [16] to evaluate the loop amplitudes. Furthermore, we apply Furry’s theorem to reduce the number of diagrams to be evaluated by a factor of two. The color factors were computed by hand and cross-checked with MADGRAPH4 [17, 18]. The numerical stability is guaranteed with the help of Ward Identities which are applied to every diagram (see Ref. [8] for details). In addition, we also generated results for this sub-process using the effective theory approximation. With this implementation, we can directly cross check our full theory results. For  $m_t = 5 \cdot 10^4$  GeV, the agreement is better than one per ten thousand level. Finally, we have cross checked successfully our results provided by the effective theory approximation with the MADGRAPH4 framework.

Both, the full and the effective theory implementation are available via the GGFLO MC program, which is a part of the VBFNLO framework [19–21].

#### 4. Numerical Results

In the following, results for integrated cross sections and differential distributions are presented at the LHC for the sub-process  $gg \rightarrow ggg\Phi$ . To cluster jets, we use the kT-algorithm and impose a minimal set of inclusive cuts to simulate experimental acceptance capabilities. Jets are required to have a  $p_T^j > 20$  GeV and to lie in the rapidity range  $|y_j| < 4.5$  with a cone radius of  $R = 0.6$ . Additionally, jets are ordered in terms of decreasing transverse momenta,  $p_T^{j_1} > p_T^{j_2} > p_T^{j_3}$ . As parton distribution functions (PDFs), we use CTEQ6L1 [22]

with  $\alpha_s(M_Z) = 0.130$ . The Higgs boson is produced on-shell and without finite width effects. As electroweak input parameters, we choose  $M_Z = 91.188$  GeV,  $M_W = 80.386$  GeV and  $G_F = 1.16637 \times 10^{-5}$  GeV $^{-2}$  and derive the weak mixing angle and the electromagnetic coupling constant using SM tree level relations. Except the top-quark with  $m_t = 173.3$  GeV and the bottom-quark with a  $\overline{\text{MS}}$  mass at  $\overline{m}_b(m_b) = 4.2$  GeV, all other participating quarks are taken to be massless. Additionally, following Refs. [12, 23], we use the relation between the pole mass and the  $\overline{\text{MS}}$  mass, within a 5-flavor scheme to take into account the evolution of  $m_b$  up to the reference scale  $m_\Phi$ . Note, that for the Higgs mass within the range of 100-1000 GeV, the Yukawa couplings contain a 33-51% smaller  $m_b$  than the pole mass of 4.855 GeV utilized in the loop propagators.

The renormalization and factorization scales, are defined by  $\alpha_s^5(\mu_R) = \alpha_s(p_T^{j_1})\alpha_s(p_T^{j_2})\alpha_s(p_T^{j_3})\alpha_s(p_\Phi)^2$  and  $\mu_F = (p_T^{j_1}p_T^{j_2}p_T^{j_3})^{1/3}$ . In the following, we present results for three different scenarios:

$$\text{H (CP-even)} : \quad \alpha = \pi/2, \quad y_q = y_q^{\text{SM}} \quad (6)$$

$$\text{A (CP-odd)} : \quad \alpha = 0, \quad \tilde{y}_q = \tilde{y}_q^{\text{II}} \quad (7)$$

$$\Phi \text{ (mixed state)} : \quad \tan \alpha = 2/3, \quad y_q = \tilde{y}_q = \tilde{y}_q^{\text{II}}. \quad (8)$$

For the effective theory approximation, we show results with and without form factors (FF). The total cross section as a function of the Higgs boson mass for the CP-even Higgs boson is presented in Fig. 2 at a center of mass energy (c.m.) of 8 TeV (left panel) and 14 TeV (right panel). As expected, bottom loop corrections are negligible within the SM. The effective theory approximation provides accurate results (10%) up to Higgs

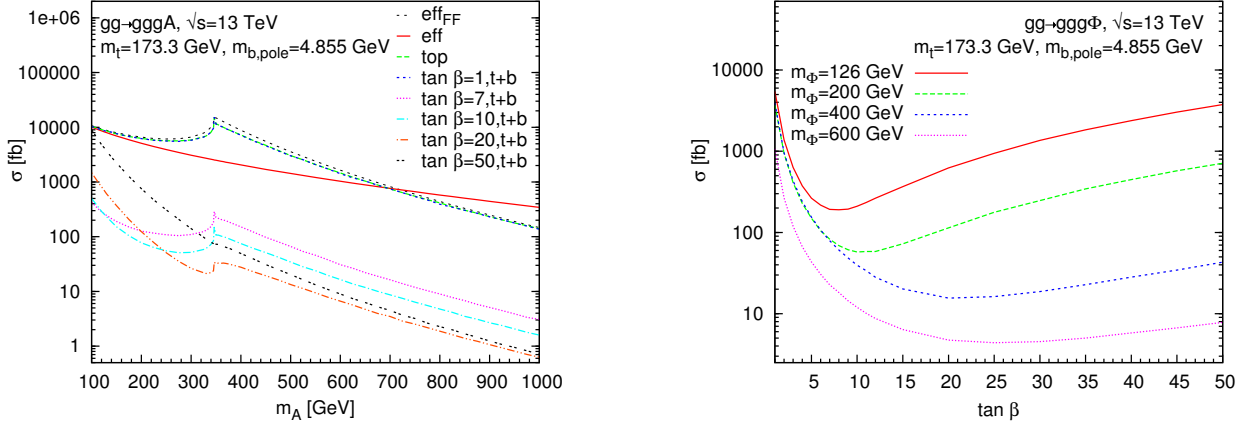


Figure 3: Left:  $A + 3$  jet cross section as a function of the pseudo-scalar Higgs boson mass  $m_A$ , for different values of  $\tan\beta$ . Right:  $\Phi + 3$  jet cross section as a function of  $\tan\beta$  for several values of  $m_\Phi$ . The applied cuts are discussed in the text.

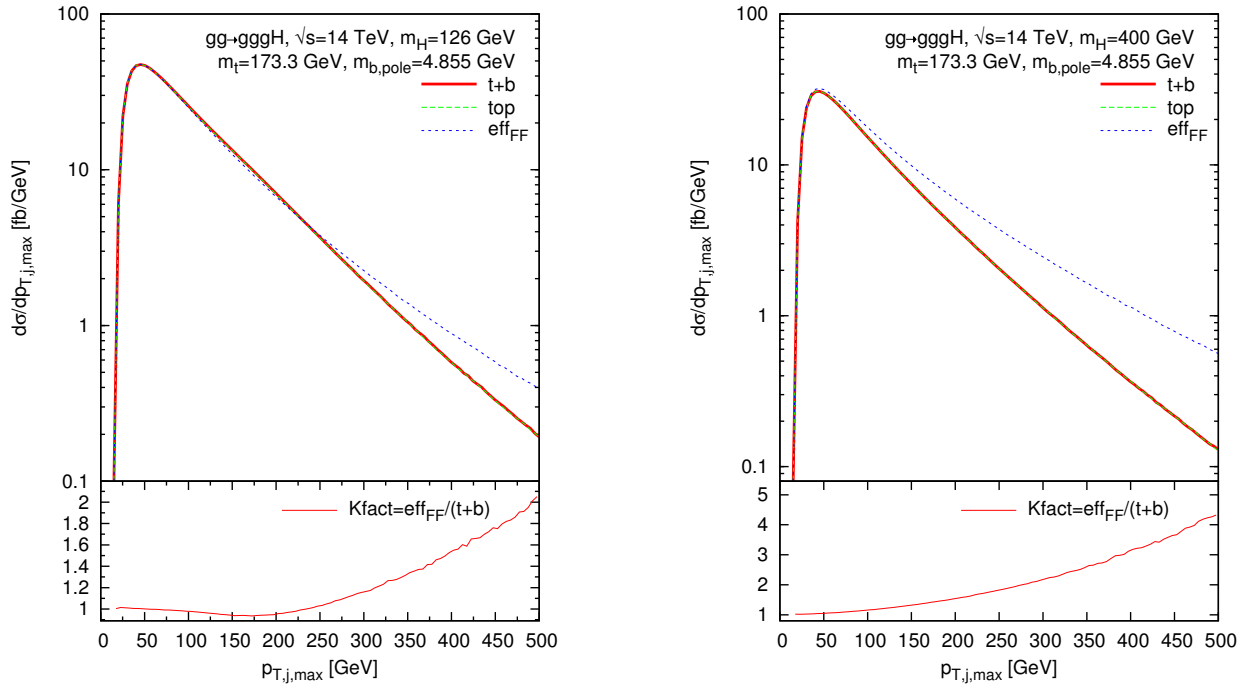


Figure 4: Comparison of transverse-momentum distributions of the hardest jet of the  $gg \rightarrow gggH$  scattering sub-process evaluated within the effective and loop-induced theory. Cuts are discussed in the text.

masses of about 150 (175) GeV at a c.m. energy of 8 (14) TeV. The application of form factors extends the validity range up to approximately 300 GeV. Additionally, it reproduces the threshold enhancement at  $m_H = 2m_t$ . Beyond 300 GeV, the total cross section is overestimated up to 20 (25) % at 8 (14) TeV c.m. energy

for  $m_H = 400$  GeV, and converges afterwards slowly to the full theory result for the shown range of the Higgs mass.

For small values of  $\tan\beta$ , similar results are obtained for a  $CP$ -odd Higgs boson (see the left panel of Fig. 3). For large values of  $\tan\beta$ , the bottom loop corrections

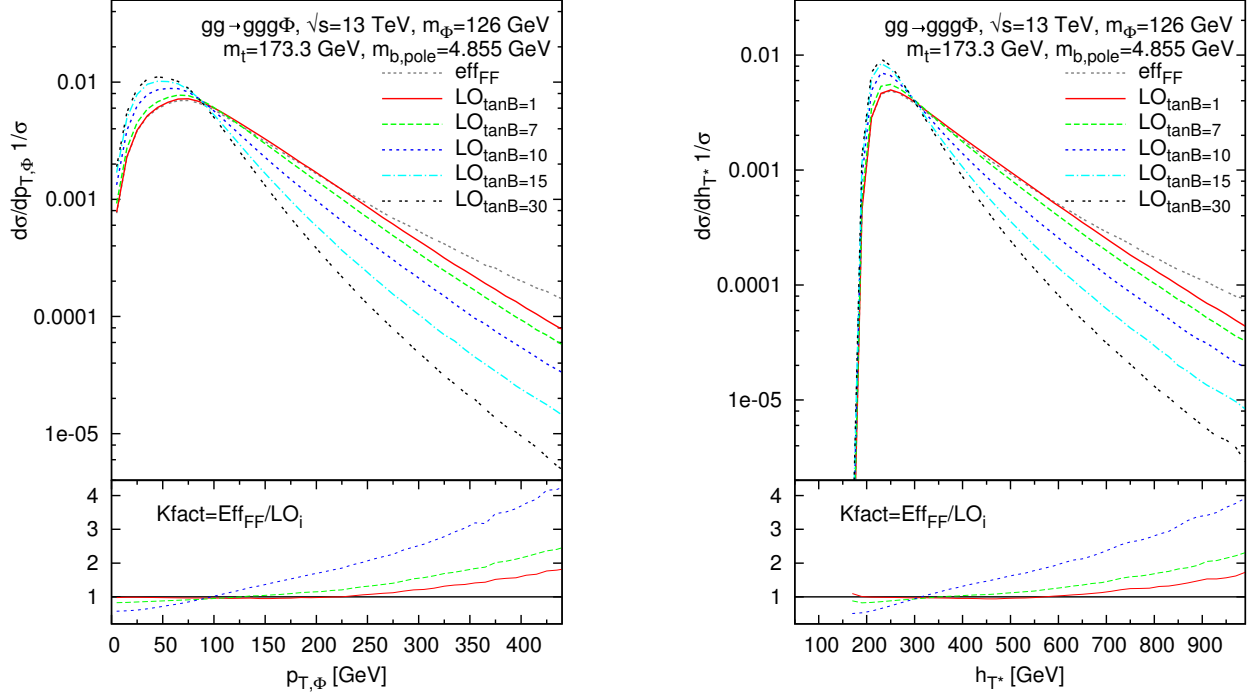


Figure 5: The transverse-momentum distributions of the Higgs boson  $\Phi$  (left panel) and the transverse scalar sum (right panel), are plotted. Details are described in the text.

dominate and the effective theory is not valid anymore. Note the fast decrease of the cross section for bottom-quark loop dominating configurations (see the  $\tan\beta = 50$  curve). For the mixed state scenario (right panel), we show the total cross section for  $\Phi jjj$  production as a function of  $\tan\beta$  for different values of the Higgs mass. Note that the minimum of the distribution, obtained for  $\tilde{y}_t^H \approx \tilde{y}_b^H$ , is shifted to larger  $\tan\beta$  values with increasing Higgs mass. This is due to the fact that the bottom-quark loop corrections decrease faster with increasing Higgs masses, hence, one needs bigger values of  $\tan\beta$  to set effectively both Yukawa couplings to equal strengths.

Next, we show selected differential distributions. In Fig. 4 the differential distribution of the transverse momentum of the leading jet is presented for a light (left) and heavy (right) Higgs boson. One can clearly see that even for light Higgs bosons large differences appear between the effective theory, including the form factors, and the full theory. The differences between both approaches are illustrated with the help of a  $K$ -factor defined as  $\text{eff}_{\text{FF}}/(t+b)$ , pictured in the lower panels. As expected, the effective theory approximation yields accurate results up to  $p_T^{\text{max}} < 200$  GeV. For a Higgs mass of 400 GeV, where the largest discrepancy is observed (about 25% at the total integration level) between the

full and the effective theory including FFs, the differences are even more prominent. The effective theory predicts harder emissions and overestimates the full theory result up to a factor of 5.

In Fig. 5, for the mixed state scenario and for small values of  $\tan\beta$ , similar effects are observed in the differential distributions of the transverse Higgs momenta (left) and the transverse scalar sum of the system (right) defined as  $h_{T^*} = \sum_i p_T^j + \sqrt{p_{T,\Phi}^2 + m_\Phi^2}$ . For  $\tan\beta = 1$ , despite the fact that the normalization is well predicted by the effective theory, large differences up to a factor of 2 appear. These discrepancies become larger with increasing values of  $\tan\beta$  and additionally stronger softening effects are visible resulting from bottom-quark loop corrections.

Next, we investigate the azimuthal angle distribution, defined as the difference of the azimuthal angle between the more-forward and the more-backward of the two tagging jets ( $\phi_{j_1 j_2} = \varphi_F - \varphi_B$ ). To increase the sensitivity of the  $\phi_{j_1 j_2}$  distribution to the  $CP$ -structure of the Higgs couplings, we slightly modify the applied cuts in the following way

$$p_T^j > 30 \text{ GeV}, \quad \Delta\eta_{j_1 j_2} > 3. \quad (9)$$

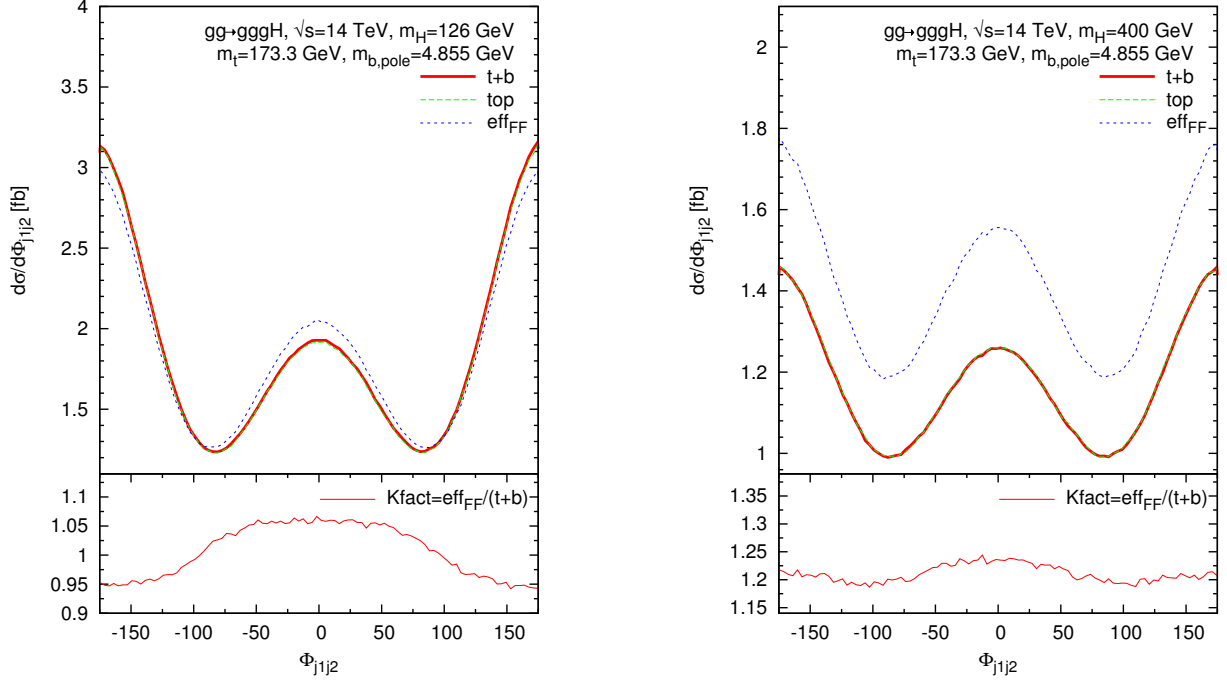


Figure 6: Comparison of the azimuthal angle distributions of the  $gg \rightarrow gggH$  scattering sub-process evaluated within the effective and loop-induced theory. Cuts are discussed in the text.

In Fig. 6, one can observe that the presence of additional soft radiation does not distort the characteristic shape obtained in the Higgs plus two jet production. In the left panel, for a 126 GeV massive Higgs boson, the effective theory approach approximates accurately the full theory with a small deviation of 5%. For a 400 GeV heavy Higgs boson, the shape is well reproduced, but 20% off in the whole spectrum. The same distribution is plotted in Fig. 7 for the  $CP$ -mixed state scenario. Here, the shift of the minimum is given by the relation,

$$\tan \Delta\phi_{j_1 j_2} = \frac{3}{2} \frac{\tilde{y}_q}{y_q} \tan \alpha. \quad (10)$$

Hence, in our model the minima are shifted to  $\phi_{j_1 j_2}^{\min} = -45^\circ, 135^\circ$ . It is clearly visible that the presence of additional radiation does not alter the main characteristics of the azimuthal angle correlations. Additionally, one observes that the effective theory approximation accurately reproduces the shape of the  $\phi_{j_1 j_2}$  distribution. However, in the full theory, it receives additionally kinematic distortions caused by the balance of the transverse momenta of the jets with respect to that of the Higgs boson due to conservation of momenta, and the softer momentum spectrum of the jets and the Higgs boson for high values of  $\tan\beta$  (see Fig. 5).

## 5. Conclusions

In these proceedings, we have presented results for the Higgs production in association with three jets. We have focused on the production process  $gg \rightarrow ggg\Phi$ , where  $\Phi$  corresponds to a general  $CP$ -violating Higgs boson, and showed results for three different scenarios. We have studied the validity of the effective theory approximation and confirmed that additional soft radiation does not alter the main characteristics of the azimuthal angle correlations. Additionally, we have shown that bottom-quark loop contributions in combination with large values of  $\tan\beta$  can lead to visible distortions of phenomenologically important differential distributions.

## 6. Acknowledgments

We thank Dieter Zeppenfeld for helpful discussions and collaborations at early stages of this project. This work was partially funded by the Deutsche Forschungsgemeinschaft via the Sonderforschungsbereich/Transregio SFB/TR-9 Computational Particle Physics. MK acknowledges support by the Grid Cluster of the RWTH-Aachen. FC acknowledges finan-

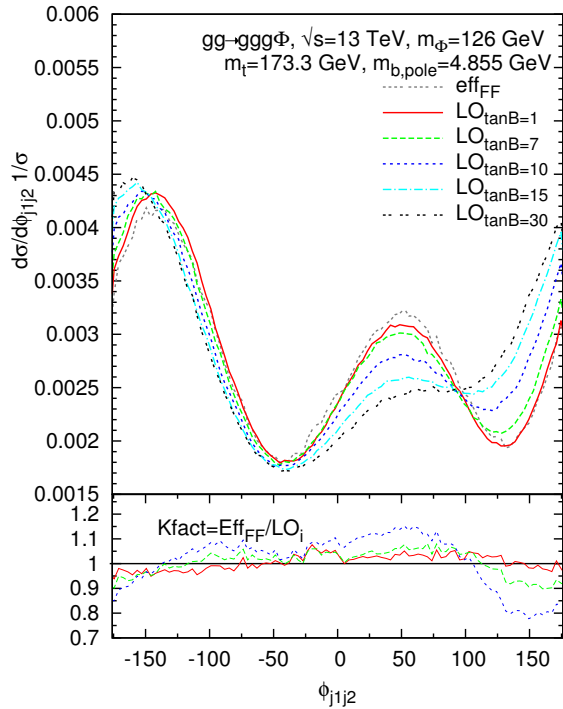


Figure 7: Azimuthal angle correlation  $\phi_{j_1j_2}$  of the two hardest jets. Cuts are discussed in the text.

cial support by the IEF-Marie Curie program (PIEF-GA-2011-298960) and partial funding by the LHCPhe-net (PITN-GA-2010-264564) and by the MINECO (FPA2011-23596).

## References

- [1] G. Aad, et al., Observation of a new particle in the search for the Standard Model Higgs boson with the ATLAS detector at the LHC, *Phys.Lett. B* 716 (2012) 1–29. [arXiv:1207.7214](#), [doi:10.1016/j.physletb.2012.08.020](#).
- [2] S. Chatrchyan, et al., Observation of a new boson at a mass of 125 GeV with the CMS experiment at the LHC, *Phys. Lett. B* 716 (2012) 30–61. 59 p. [arXiv:1207.7235](#).
- [3] V. Del Duca, W. Kilgore, C. Oleari, C. Schmidt, D. Zeppenfeld, Higgs + 2 jets via gluon fusion, *Phys.Rev.Lett.* 87 (2001) 122001. [arXiv:hep-ph/0105129](#), [doi:10.1103/PhysRevLett.87.122001](#).
- [4] K. Odagiri, On azimuthal spin correlations in Higgs plus jet events at LHC, *JHEP* 0303 (2003) 009. [arXiv:hep-ph/0212215](#).
- [5] F. Campanario, M. Kubocz, D. Zeppenfeld, Gluon-fusion contributions to Phi + 2 Jet production, *Phys.Rev. D* 84 (2011) 095025. [arXiv:1011.3819](#), [doi:10.1103/PhysRevD.84.095025](#).
- [6] J. M. Campbell, R. K. Ellis, G. Zanderighi, Next-to-Leading order Higgs + 2 jet production via gluon fusion, *JHEP* 0610 (2006) 028. [arXiv:hep-ph/0608194](#), [doi:10.1088/1126-6708/2006/10/028](#).
- [7] H. van Deurzen, N. Greiner, G. Luisoni, P. Mastrolia, E. Mirabella, et al., NLO QCD corrections to the production of Higgs plus two jets at the LHC, *Phys.Lett. B* 721 (2013) 74–81. [arXiv:1301.0493](#), [doi:10.1016/j.physletb.2013.02.051](#).
- [8] F. Campanario, M. Kubocz, Higgs boson CP-properties of the gluonic contributions in Higgs plus three jet production via gluon fusion at the LHC [arXiv:1402.1154](#).
- [9] F. Campanario, M. Kubocz, Higgs boson production in association with three jets via gluon fusion at the LHC: Gluonic contributions, *Phys.Rev. D* 88 (2013) 054021. [arXiv:1306.1830](#), [doi:10.1103/PhysRevD.88.054021](#).
- [10] G. Cullen, H. van Deurzen, N. Greiner, G. Luisoni, P. Mastrolia, et al., NLO QCD corrections to Higgs boson production plus three jets in gluon fusion, *Phys.Rev.Lett.* 111 (2013) 131801. [arXiv:1307.4737](#), [doi:10.1103/PhysRevLett.111.131801](#).
- [11] F. Campanario, T. Figy, S. Platzer, M. Sjoedahl, Electroweak Higgs plus Three Jet Production at NLO QCD, *Phys.Rev.Lett.* 111 (2013) 211802. [arXiv:1308.2932](#), [doi:10.1103/PhysRevLett.111.211802](#).
- [12] M. Spira, QCD effects in Higgs physics, *Fortsch.Phys.* 46 (1998) 203–284. [arXiv:hep-ph/9705337](#).
- [13] A. Djouadi, The Anatomy of electro-weak symmetry breaking. II. The Higgs bosons in the minimal supersymmetric model, *Phys.Rept.* 459 (2008) 1–241. [arXiv:hep-ph/0503173](#), [doi:10.1016/j.physrep.2007.10.005](#).
- [14] F. Campanario, Q. Li, M. Rauch, M. Spira, ZZ+jet production via gluon fusion at the LHC, *JHEP* 1306 (2013) 069. [arXiv:1211.5429](#), [doi:10.1007/JHEP06\(2013\)069](#).
- [15] F. Campanario, Towards  $pp \rightarrow VVjj$  at NLO QCD: Bosonic contributions to triple vector boson production plus jet, *JHEP* 1110 (2011) 070. [arXiv:1105.0920](#), [doi:10.1007/JHEP10\(2011\)070](#).
- [16] K. Hagiwara, D. Zeppenfeld, Helicity Amplitudes for Heavy Lepton Production in  $e^+ e^-$  Annihilation, *Nucl.Phys. B* 274 (1986) 1. [doi:10.1016/0550-3213\(86\)90615-2](#).
- [17] J. Alwall, P. Demin, S. de Visscher, R. Frederix, M. Herquet, et al., MadGraph/MadEvent v4: The New Web Generation, *JHEP* 0709 (2007) 028. [arXiv:0706.2334](#), [doi:10.1088/1126-6708/2007/09/028](#).
- [18] J. Alwall, M. Herquet, F. Maltoni, O. Mattelaer, T. Stelzer, MadGraph 5 : Going Beyond, *JHEP* 1106 (2011) 128. [arXiv:1106.0522](#), [doi:10.1007/JHEP06\(2011\)128](#).
- [19] K. Arnold, M. Bahr, G. Bozzi, F. Campanario, C. Englert, et al., VBFNLO: A Parton level Monte Carlo for processes with electroweak bosons, *Comput.Phys.Commun.* 180 (2009) 1661–1670. [arXiv:0811.4559](#), [doi:10.1016/j.cpc.2009.03.006](#).
- [20] K. Arnold, J. Bellm, G. Bozzi, M. Brieg, F. Campanario, et al., VBFNLO: A Parton Level Monte Carlo for Processes with Electroweak Bosons – Manual for Version 2.5.0 [arXiv:1107.4038](#).
- [21] K. Arnold, J. Bellm, G. Bozzi, F. Campanario, C. Englert, et al., Release Note – Vbfnlo-2.6.0 [arXiv:1207.4975](#).
- [22] J. Pumplin, D. Stump, J. Huston, H. Lai, P. M. Nadolsky, et al., New generation of parton distributions with uncertainties from global QCD analysis, *JHEP* 0207 (2002) 012.
- [23] J. Vermaseren, S. Larin, T. van Ritbergen, The four loop quark mass anomalous dimension and the invariant quark mass, *Phys.Lett. B* 405 (1997) 327–333. [arXiv:hep-ph/9703284](#), [doi:10.1016/S0370-2693\(97\)00660-6](#).